Heliyon 5 (2019) e02421

Contents lists available at ScienceDirect

Heliyon

journal homepage: www.heliyon.com

Heliyon

Interlayer structure and magnetic field-induced orientation of modified nanoclays in polymer aqueous solution

Min Kwan Kang [a], Eun Jung Cha [b], Hyun Hoon Song [b], Yang Ho Na [b,*]

[a] Reliability Assessment Center, Korea Research Institute of Chemical Technology, Daejeon, 34114, Republic of Korea
[b] Department of Advanced Materials, Hannam University, Daejeon, 34054, Republic of Korea

ARTICLE INFO

Keywords:
Materials science
Montmorillonite
Magnetic field
Orientation
Interlayer structure
Small angle X-ray scattering

ABSTRACT

Structural changes and orientation of organically modified montmorillonite (Mt) were investigated by employing synchrotron small-angle X-ray scattering. Mt was modified with various cationic compound [3-(methacryloylamino)propyl]-trimethyl ammonium chloride (MPTC) contents (1.5, 3, 6, 12, and 18 CEC (cation exchange capacity) per 1 CEC of Mt). There are two types of modified Mt structures, lateral monolayer and paraffin type monolayer, in accordance with the MPTC contents. A paraffin-type monolayer is more dominant than a lateral monolayer for efficient packing of MPTC between Mt layers as the MPTC contents increase. In 10 wt % of the modified Mt series oriented in 1 M of polyacrylamide aqueous solution using a magnetic field (1.2 Tesla), the modified Mt series oriented parallel to the magnetic field within 200 s.

1. Introduction

Inorganic and organic nanoparticles (NPs) have attracted considerable attention in chemical (Liu et al., 2015; Kitajima et al., 2013), physical (Kojima et al., 1993a, 1993b; Schexnailder and Schmidt, 2009), and biological applications (Greenland, 1963) over the decades. It is because of the advantage of being able to control easily the microstructure in designing suitable engineering materials at the nanoscale level. Studies for well-controlled arrangement and distribution of NPs have been effective in improving the thermal (Rao and Blanton, 2008), electronic (Kitajima et al., 2013; Park et al., 2006), and mechanical properties of nanocomposites (Giannelis et al., 1999; Alexandre and Dubois, 2000; Choi et al., 2004). The control of NP structures is important in regard to achieving superb effectiveness in their use as a minimum filler. The precise morphological control of NPs enables the application of high functionality in, for example, engineered aerospace structures, electronic materials, and optical grating.

Montmorillonite (Mt) belongs to aluminum silicate clays of the smectite group and is known to have useful properties in polymer nanocomposites. A 2:1 type layered silicate of Mt consists of an octahedral alumina or magnesia sheet sandwiched between two tetrahedral sheets (Pinnavaia, 1983). The silica sheets bond with positive ions such as Na^+, Ca^{2+}, or K^+ on their surfaces. Mt has a high surface charge, cation exchange capability, and large specific surface area. Mt in clay-polymer nanocomposites also provides a large contact surface between the polymer and clay. The polymer-clay nanocomposites can be greatly improved in terms of mechanical properties (Lan and Pinnavaia, 1994; Sheng et al., 2004; Buxton and Balazs, 2002), dimensional stability (Gusev and Lusti, 2001), and thermal resistance (Rao and Blanton, 2008). However, Mt is incompatible with many hydrophobic polymers because of the presence of the positive ions, hydrophilic surface, and strong interaction between the layers. The organophilicity of the clay can be increased by exchange of the positive ions with organic cations or surfactant treatment (Yano et al., 1993; Gilman et al., 2000). The space between the layers of ion-exchanged Mt also increases. The ion-exchanged Mt can help the process of not only hydrophilic but also hydrophobic polymer chain intercalation within the clay mineral layer. At this time, the molar characteristics of ion-exchanged surfactants, such as the amount and length of substitute molecules, affects the Mt structure (Wang et al., 2001; Lagaly, 1979, 1981; 1986; Zanetti et al., 2002). By using X-ray diffraction and FTIR, Richard reported that layer space decreases as the chain packing density decreases and the available specific surface area of the molecule increases (Vaia et al., 1994). The dependence of the interlayer structure on the chain length of primary alkyl amines ($C_nH_{2n+1}NH_2$) was shown by a lateral monolayer appearing for $n = 6$, lateral bilayer for $n = 9$–12, and paraffin-type monolayer for $n = 13$–18 (Vaia et al., 1994).

In the nanofilled systems, the oriented nanoparticle is considered as important for substantial improvements in mechanical (Sheng et al.,

* Corresponding author.
E-mail address: yhna@hnu.kr (Y.H. Na).

https://doi.org/10.1016/j.heliyon.2019.e02421
Received 14 May 2019; Received in revised form 15 July 2019; Accepted 2 September 2019

2004; Buxton and Balazs, 2002), barrier (Gusev and Lusti, 2001), electrical (Liu et al., 2015), and thermal properties (Rao and Blanton, 2008) in comparison with random dispersions. Some researchers reported Mt oriented parallel or perpendicular to the film surface in clay composites by a strong magnetic field, and the oriented clay composites indicated different conductivity along the orientation direction of Mt (Kitajima et al., 2013; Koerner et al., 2004, 2005). Here, the orientation by magnetic field (Fischer et al., 2003), is valuable because of its nondestructive nature compared with mechanical shearing (Sun et al., 2009) and electric fields (Kim et al., 2003; Park et al., 2006), and it is particularly suitable for high-aspect-ratio materials, such as clays, fibers, and polymers (Velev, 2004).

Therefore the structural characteristics of Mt in a solution media can be controlled through the relationship with cationic compound and the modified Mts are expected to have a significant impact on compatibility with polymer matrices. Furthermore, it is necessary to study the orientation of Mt as a basic research for improving the mechanical properties of polymer nanocomposites. Here we have conducted a study on the orientation and modification of Mt as a preliminary step in the structural research of aligned polymer nanocomposites. In this study, [3-(methacryloylamino)propyl]-trimethyl ammonium chloride (MPTC) was used as a cation compound. Modified Mt is a structure in which MPTC is intercalated between Mt layers. The structure of the modified Mt powder with various concentrations of MPTC was investigated by using a synchrotron X-ray beam. The orientation process of the modified Mt series in magnetic fields was obtained by X-ray measurements in real-time, and the structural arrangements of cation monomers between the clay mineral layer and the orientation of the modified Mt by magnetic field were confirmed.

2. Experimental

2.1. Preparation of modified Mt nanoclay

Dried Na^+-Mt (Cloisite-Na+, BMK Additives & Instruments) of 3 g was dispersed in 100 ml water with (3-(methacryloylamino)propyl)-trimethyl ammonium chloride (MPTC 50wt% solution in H_2O, Sigma-Aldrich) for 24 h to enable exchange of sodium to MPTC. The cation exchange capacity (CEC) of Na^+-Mt is 75.2 mequiv/100 g. Here, the various MPTC concentrations were 1.5, 3, 6, 12, and 18 CEC based on Mt 1 CEC. A centrifugation process was repeated three times to obtain the modified Mt clay. The modified Mt powder was obtained below 53 μm by sifting after freeze-drying at room temperature for 24 h. The modified nanoclays with an MPTC content of 1.5 CEC, 3 CEC, 6 CEC, 12 CEC, and 18 CEC are referred to as M-M1.5, M-M3, M-M6, M-M12, and M-M18, respectively.

2.2. Thermal analysis

Thermal stability of the modified Mt was examined by thermal gravimetric analysis (TGA; TGA N-1000, Scinco Co., Ltd) under a nitrogen gas atmosphere. The heating rate was done at 20 °C/min from 25 °C to 800 °C. From the results of TGA displayed in Fig. 1, water evaporation at 100 °C and the thermal degradation of MPTC at 200–600 °C were confirmed. A quantitative comparison can not be made since it is difficult to distinguish between MPTC and Mt, but the decomposition mass tends to increase with increasing MPTC content.

2.3. Modified Mt in polyacrylamide aqueous solution for orientation

Of the modified Mt, 10 wt% was dispersed by sonication in 1 M of polyacrylamide (400,000–800,000 g/mol, Tokyo Chemical Industry Co., Ltd.) aqueous solution. The orientation of the modified Mt by a magnetic field was carried out in the polyacrylamide solution. A permanent magnet with a strength of 1.2 Tesla was used for the orientation. The magnetic field was applied to the solution at room temperature for 15 min.

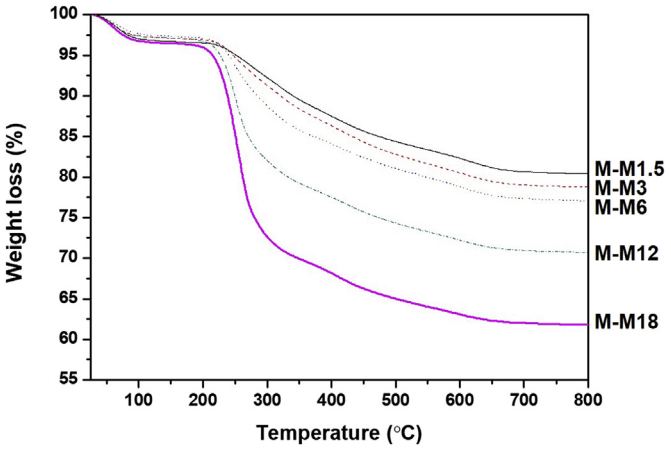

Fig. 1. TGA profile of the modified Mt nanoclays with different MPTC content.

2.4. SAXS measurements for the structural analysis of layered nanoclays

Small angle X-ray scattering (SAXS) measurements were carried out at the 4C beam-line in the Pohang Accelerator Laboratory (PAL) in South Korea. Beam energy was 19.6 keV (wavelength: 0.633 Å) and exposure time was 15 s. The two-dimensional (2D) SAXS patterns were recorded by a CCD detector (Rayonix SX165, USA). Sample-to-detector distances were fixed at 0.5 m. The scattering angles for SAXS were calibrated by silver behenate. Aluminum (Al) holder (thickness: 1 mm) with an Al foil cover (thickness: 15 μm) was used. The holder was placed on the magnet as shown in Fig. 2a and X-ray measurements were carried out every 20 s for 15 min.

2.5. Orientation parameter

Herman's orientation parameter (f) was used to determine the orientation of the Mt nanoclays induced by magnetic field in the polyacrylamide aqueous solution. Herman's orientation parameter can be defined as (Alexander, 1969; Patil et al., 2009; Chu et al., 2014):

$$f = \frac{3 < \cos^2 \Phi > - 1}{2} \quad (1)$$

The term $<\cos^2 \Phi>$ can be calculated by:

$$< cos^2\Phi > = \frac{\int_0^{\frac{\pi}{2}} I(\Phi) cos^2\Phi sin\Phi d\Phi}{\int_0^{\frac{\pi}{2}} I(\Phi) sin\Phi d\Phi} \quad (2)$$

where $I(\Phi)$ is the intensity distribution around the azimuthal angle at maximum scattering intensity, as shown in Fig. 2a. The intensity values used in the calculation for Herman's orientation parameter are taken azimuthally in an anticlockwise direction from the azimuthal angle 0°–90°. For perfect parallel and perpendicular orientation regarding the magnetic field direction, the values are 1 and -0.5, respectively. The value is 0 when Mt clay is randomly oriented.

3. Results and discussion

3.1. Structure of layered MPTC-modified Mt nanoclays

Modification of Mt is an important process in the application of clay as a filler in a polymer matrix or cross-linking agents in hydrogel. A *d*-value of the modified Mt generally increases by the intercalation of the cation monomer, which can be observed by small angle X-ray scattering. SAXS images of Na^+-Mt and the modified Mts with various MPTC contents (1.5 CEC, 3 CEC, 6 CEC, 12 CEC, 18 CEC) are shown in Fig. 3a. All the samples, except for M-M18, clearly show the ring patterns, which

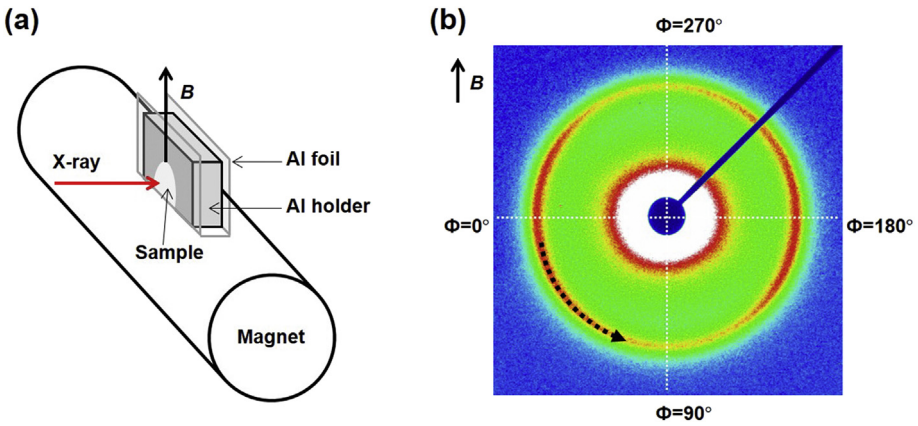

Fig. 2. (a) Scheme of the sample holder for SAXS measurements. The direction of a magnetic field is perpendicular to the magnet at the measuring point. (b) The determination of Herman's orientation factor (f) using two-dimensional SAXS patterns. The integrated intensity corresponding to $\Phi = 0°–90°$ was used to obtain the orientation parameter.

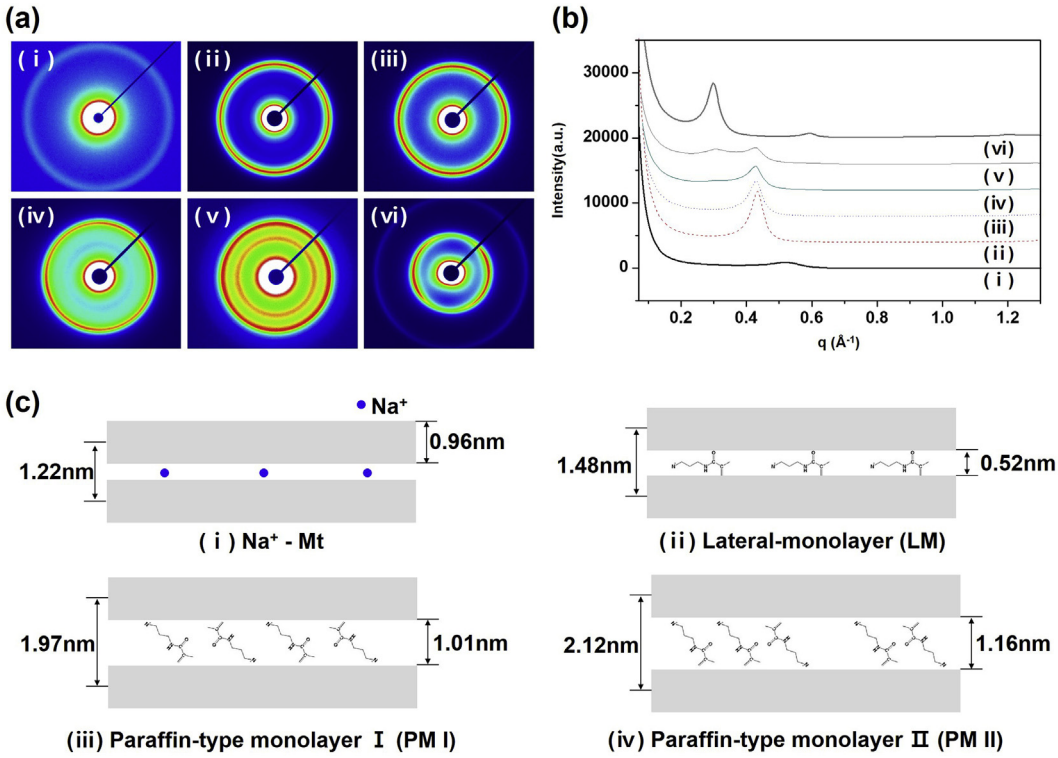

Fig. 3. (a) SAXS images of (i) Na^+-Mt, (ii) M-M1.5, (iii) M-M3, (iv) M-M6, (v) M-M12, and (vi) M-M18. (b) 1-D scattering intensity profiles from the SAXS images. (c) The structure of Na^+-Mt and MPTC-modified Mt nanoclays.

indicate the random orientation of the modified Mt plates. The X-ray scattered intensity of M-M18 in Fig. 3a-vi concentrates to the equator, indicating the orientation of the modified Mt nanoclay. It is believed to be a "preferred orientation" caused by the shape of the particles. It can be very difficult for the microcrystal like plate or needle shapes in the powder sample to form random orientation because of the tendency for the crystallites to be oriented in one way (Ho et al., 1999). The modified Mt having the plate-like shapes is also considered to be oriented in a particular direction. The preferred orientation controlled by gravity sedimentation, the suction method, and dry pressing has been studied for the orientation of clays such as kaolinite and illite (Niskanen, 1964; Gibbs, 1965; Zevin and Viaene, 1990). In addition, studies on inducing the orientation of the polymer on the clay surface have also been reported using the preferred orientation of clay-polymer composites (Rao and Blanton, 2008; Li and Zhao, 2011; Chu et al., 2014).

1-D intensity profiles derived from the SAXS images in Fig. 3a are illustrated in Fig. 3b. The q value ($q = 2\pi/d$-value) of the reflection becomes smaller with the increase of MPTC content. The unmodified Na^+-Mt shows a weak reflection of (001) at 0.51 $Å^{-1}$ corresponding to a d-value of 1.22 nm (Fig. 3b-i). The modified Mt nanoclays of (ii), (iii), (iv), and (v) show a reflection at 0.43 $Å^{-1}$ corresponding to a d-value of 1.48 nm, which was smaller than that of the unmodified Mt. The reflected intensity at 0.43 $Å^{-1}$ decreased with the increase in MPTC content. In addition, a reflection at 0.32 $Å^{-1}$ corresponding to a d-value of 1.97 nm is shown in (iv) and (v), and the intensity of this reflection increases with MPTC content. On further increase of MPTC content, the reflection at 0.43 $Å^{-1}$ disappears, but the reflections at 0.30 $Å^{-1}$ and 0.59 $Å^{-1}$ appear in (vi) (the d-value is 2.12 nm and 1.06 nm, respectively). Here, the

Table 1
Arrangement types of MPTC-modified Mt nanoclays.

Sample	Type
M-M1.5	LM
M-M3	LM
M-M6	LM, PMI
M-M12	LM, PMI
M-M18	PMII

reflection at 0.59 $Å^{-1}$ represents the (002) plane. The *d*-value of the modified Mts increases with the increase in MPTC content (1.48 < 1.97 < 2.12 nm), indicating that the structural change of the layered Mt nanoclays depends on the intercalation of MPTC molecules.

The changes of the *d*-value are attributed to the arrangement and the length of the cation monomer intercalated between Mt layers. The *d*-value of the organosilicate clays, which are synthesized by a cation-exchange reaction between Li^+-fluorohectorite and excess alkylammonium salt, also increases as the alkyl chain length increases (Vaia et al., 1994). The lateral monolayer, bilayer, and paraffin-type structures were shown in accordance with the number of carbons, 6, 9, and 13, respectively.

The layered structure of the modified Mt is closely related to the structure and the amount of the intercalated MPTC molecules. The MPTC molecule consists of two parts, a head group of three methyls and a body group of an alkyl chain. The length of the MPTC chain is about 1.56 nm and the thickness is about 0.51 nm. As shown in Fig. 3c-i, the thickness of Na^+-Mt is about 0.96 nm (Choi et al., 2004). Our results from the SAXS data suggest that the structure of Na^+-Mt and the MPTC-modified Mt can be roughly classified into two types, lateral monolayer (LM) and paraffin type-monolayer (PM I and PM II) (Fig. 3c). The MPTC monomer in M-M1.5 and M-M3 is parallel to the Mt surface, as shown by the LM in Fig. 3c-ii, based on the interlayer space being 0.52 nm. The M-M6 and M-M12 with larger interlayers than the MPTC thickness show the PM I structure (Fig. 3c-iii). The MPTC molecule in this paraffin-type

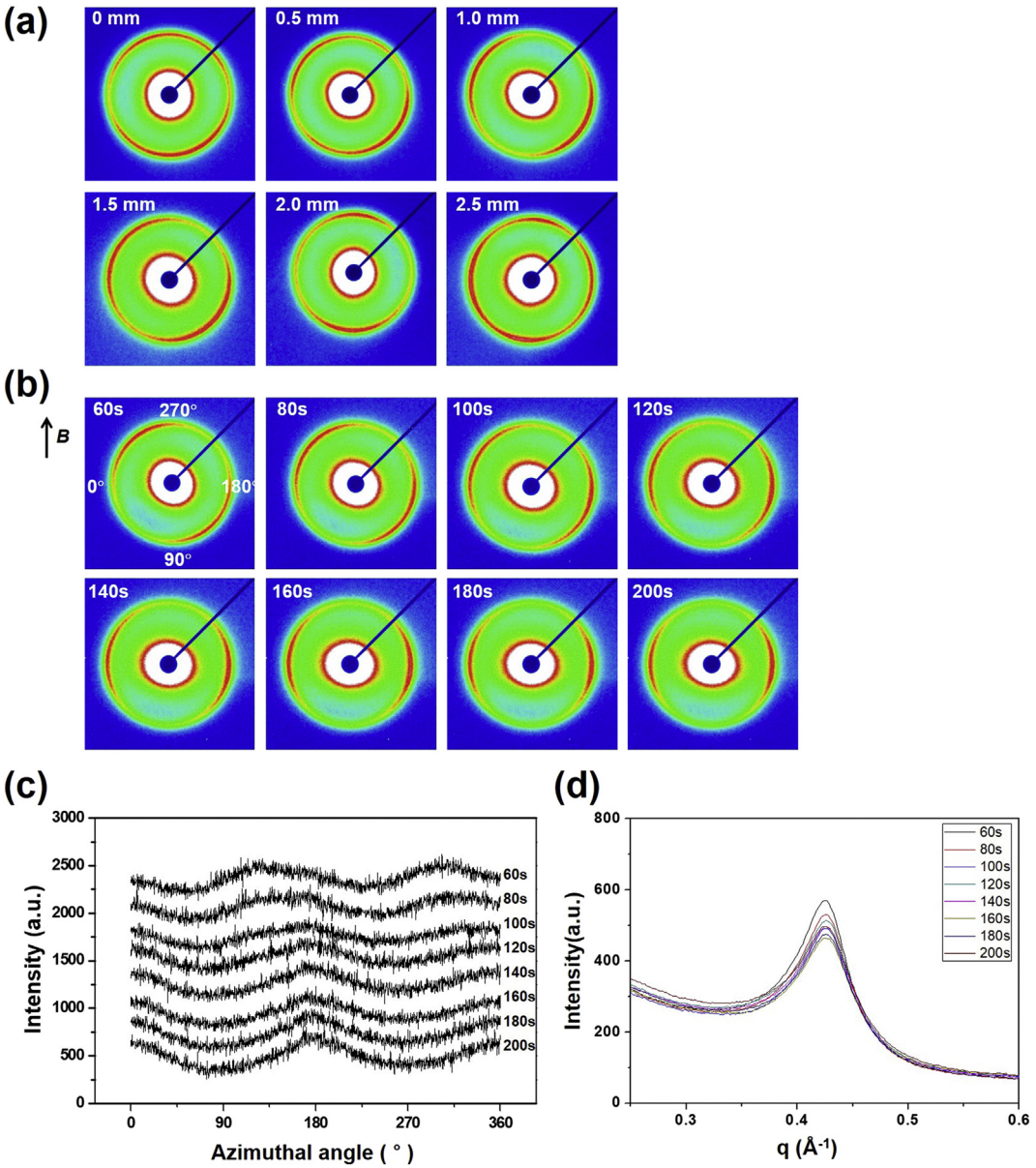

Fig. 4. (a) SAXS images of M-M3 when measuring point of the X-ray changes every 0.5 mm. (b) Change in SAXS images of M-M3 sample over time under a magnetic field. (c) Azimuthal scattering intensity of the M-M3 sample over time under a magnetic field. (d) 1-D scattering intensity profiles of the M-M3 sample over time under magnetic field.

monolayer is tilted to the Mt surface. In addition, the two reflections in the SAXS data of M-M6 and M-M12 indicate the coexistence of both LM and PM I structures. The tilted angle of PM II in M-M18 is larger than PM I. The reflection of (002) the plane on M-M18 means the high order of the PM II structure, but the LM type is not detected. The arrangement types of the MPTC-modified Mt nanoclays are shown in Table 1. LM of the modified Mt changes into PM with the increase in the intercalated MPTC content. It is noteworthy that MPTC molecules between the Mt layers arrange in tilted states for effective packing.

3.2. Orientation of MPTC-modified Mt nanoclays by magnetic field

M-M nanoclays were dispersed in the polyacrylamide aqueous solution. Here, to maintain stably the orientation of the layered M-M nanoclays, 1 M polyacrylamide aqueous solution was selected to provide appropriate viscosity in this system. The direction of orientation of M-M3 changes irregularly when the measuring point of the X-ray changes every 0.5 mm without the magnetic field as displayed in Fig. 4a. The SAXS images of M-M3 in the polyacrylamide aqueous solution showed oriented patterns similar to those of the M-M18 powder that were attributed to the preferred orientation (Fig. 3a-vi). However, it was found that each domain of M-M3 was randomly oriented in the polymer aqueous solution. These polydomain structures can be also shown in polymeric elastomers with liquid crystal structures, which combine the anisotropy of liquid crystals with the elasticity of polymer networks (Ortiz et al., 1998; Hiraoka et al., 2004; Urayama et al., 2009; Na et al., 2014).

The real-time X-ray scattering images for the M-M3 sample in the polyacrylamide aqueous solution measured under a magnetic field of 1.2 Tesla are shown in Fig. 4b. Here, the direction of the magnetic field is perpendicular to the image. In the image measured at 60 s, the center of the reflection is observed at about 140° (320°). It can be seen that the scatter pattern moves in the equatorial direction over time (the images after 200 s are not shown). That is, the surface of M-M3 is oriented in a direction parallel to the direction of the magnetic field. Although the image at 60 s for each sample shows different orientations, which correspond to the preferred orientation, it clearly shows that the surface of M-M3 moves in a direction parallel to the direction of the magnetic field. The nanoclay within the magnetic field shows the universal alignment response of clay plates with the principal axis parallel to or perpendicular to the magnetic field. For example, a 6 wt % concentration of a Southern Clay Mt (Cloisite NA, 92 mequiv/100 g) exchanged with octadecylammonium halides in epoxy (Epon 862/W) nanocomposites was oriented by a 1.2 Tesla magnet field for about 10 min (Koerner et al., 2005). The result of this study shows about three times faster orientation although the solution media is different.

The position of the reflection can be confirmed in detail through the azimuthal intensity profiles obtained from each scattering pattern (Fig. 4c). The reflection is observed at around 140° (320°) in 60 s and then moves with time to finally near 180° (360°) in 200 s. This phenomenon was reproducible in repeated experiments under the same condition. These results clearly show that the M-M3 nanoclay is rotated by the magnetic field and oriented parallel to the direction of the magnetic field. Here, the interlayer distance is fixed to 1.48 nm, so that there is no influence of the magnetic field on the interlayer distance (Fig. 4d).

The change of the angle of the reflection over time from the difference of the azimuthal angle 0° is shown in Fig. 5a. The data for M-M1.5 at 60 s and 80 s could not be obtained experimentally because the azimuthal intensity distribution was very heterogeneous. For M-M1.5 and M-M6, the surface direction of the MPTC-modified clay was initially parallel to the direction of the magnetic field at 60 s, but the data for M-M3, M-M12, and M-M18 gradually converged to 0, and the orientation direction changed parallel to the magnetic field. The tendency was also evident in the orientation parameters, although the value change was small. The orientation parameter value was close to the value of 0 indicating isotropy at 60 s, and it gradually increased so that the scattering intensity was concentrated in the equatorial direction, that is, in a direction parallel to the direction of the magnetic field (Fig. 5b).

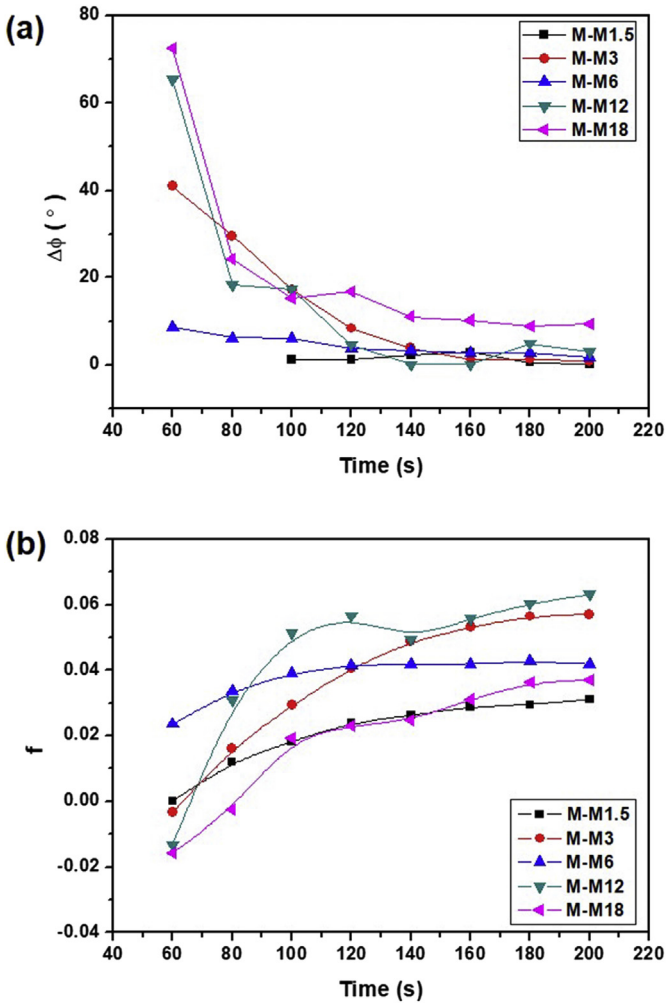

Fig. 5. (a) Change of the angle of the peak position from the difference of the azimuthal angle 0° and (b) change of the orientation parameter over time.

4. Conclusion

Mt clay was organically modified, and structural change with intercalation by MPTC and orientation by a magnetic field in an aqueous polymer solution were investigated based on X-ray scattering experiments. From the results, it can be assumed that MPTC penetrates between the clay mineral layers and shows a lateral monolayer parallel to the Mt surface and two paraffin type monolayer structures with inclined angles. The monolayers with various structures were seen at different levels of MPTC content. The lateral monolayer was shown at the low level of MPTC content, and the monolayer and MPTC were present at the same level as the paraffin type monolayer for efficient packing. Above this level, only the paraffin type monolayer was present, and the inclination angle of MPTC further increased. The orientation of MPTC-Mt on the aqueous polymer solution was locally different. However, this orientation changes in a direction parallel to a magnetic field when under the magnetic field. Also, regardless of the structure of the MPTC-Mt, it tends to align in a direction parallel to the direction of the magnetic field under a magnetic field. These changes occur at about 200 s or less and show that MPTC-Mt can be rapidly oriented in aqueous polymer solution even at a relatively weak 1.2 Tesla. Further study on the characteristics of the oriented polymer gels using modified Mt by cationic organic material as a cross-linking agent are in progress.

Declarations

Author contribution statement

Yang Ho Na: Conceived and designed the experiments; Analyzed and interpreted the data; Wrote the paper.

Min Kwan Kang: Performed the experiments; Analyzed and interpreted the data; Wrote the paper.

Eun Jung Cha: Performed the experiments.

Hyun Hoon Song: Conceived and designed the experiments.

Funding statement

This work was supported by a National Research Foundation of Korea (NRF) grant funded by the Ministry of Education (NRF-2018R1D1A1B07043881) and partially supported by the 2019 Hannam University Research Fund.

Competing interest statement

The authors declare no conflict of interest.

Additional information

No additional information is available for this paper.

Acknowledgements

The X-ray experiment was performed at the 4C beam line in the Pohang Accelerator Laboratory.

References

Alexander, L.E., 1969. X-ray Diffraction Methods in Polymer Science. John Wiley & Sons, New York.

Alexandre, M., Dubois, P., 2000. Polymer-layered silicate nanocomposites: preparation, properties and uses of a new class of materials. Mater. Sci. Eng. R Rep. 28, 1–63.

Buxton, G.A., Balazs, A.C., 2002. Lattice spring model of filled polymers and nanocomposites. J. Chem. Phys. 117, 7649–7658.

Choi, Y.S., Ham, H.T., Chung, I.J., 2004. Effect of monomers on the basal spacing of sodium montmorillonite and the structures of polymer-clay nanocomposites. Chem. Mater. 16, 2522–2529.

Chu, C.-Y., Chen, M.-H., Wu, M.-L., Chen, H.-L., Chiu, Y.-T., Chen, S.-M., Huang, C.-H., 2014. Hierarchical structure and crystal orientation in poly(ethylene oxide)/clay nanocomposite films. Langmuir 30, 2886–2895.

Fischer, J.E., Zhou, W., Vavro, J., Llaguno, M.C., Guthy, C., Haggenmueller, R., Casavant, M.J., Walters, D.E., Smalley, R.E., 2003. Magnetically aligned single wall carbon nanotube films: preferred orientation and anisotropic transport properties. J. Appl. Phys. 93, 2157–2163.

Giannelis, E.P., Krishnamoorti, R., Manias, E., 1999. Polymer-silicate nanocomposites: model systems for confined polymers and polymer brushes. Adv. Polym. Sci. 138, 107–147.

Gibbs, R.J., 1965. Error due to segregation in quantitative clay mineral X-ray diffraction mounting techniques. Am. Mineral. 50, 741–751.

Gilman, J.W., Jackson, C.L., Morgan, A.B., Harris, R., Manias, E., Giannelis, E.P., Wuthenow, M., Hilton, D., Phillips, S.H., 2000. Flammability properties of polymer-layered-silicate nanocomposites, polypropylene and polystyrene nanocomposites. Chem. Mater. 12, 1866–1873.

Greenland, D.J., 1963. Adsorption of polyvinyl alcohols by montmorillonite. J. Coll. Sci. 18, 647–664.

Gusev, A.A., Lusti, H.R., 2001. Rational design of nanocomposites for barrier applications. Adv. Mater. 13, 1641–1643.

Hiraoka, K., Stein, P., Finkelmann, H., 2004. Electromechanics of a chiral smectic C elastomer: measurement of complex piezoelectric constant through successive phase transformations. Macromol. Chem. Phys. 205, 48–54.

Ho, N.-C., Peacor, D.R., Pluijm, B.A., 1999. Preferred orientation of phyllosilicates in Gulf Coast mudstones and relation to the smectite-illite transition. Clay Miner. 47, 495–504.

Kim, D.H., Park, J.U., Ahn, K.H., Lee, S.J., 2003. Electrically activated poly(propylene)/clay nanocomposites. Macromol. Rapid Commun. 24, 388–391.

Kitajima, S., Matsuda, M., Yamato, M., Tominaga, Y., 2013. Anisotropic ionic conduction in composite polymer electrolytes filled with clays oriented by a strong magnetic field. Polym. J. 45, 738–743.

Koerner, H., Jacobs, D., Tomlin, D.W., Busbee, J.D., Vaia, R., 2004. Tuning polymer nanocomposite morphology: AC electric field manipulation of epoxy-montmorillonite (clay) suspensions. Adv. Mater. 16, 297–302.

Koerner, H., Hampton, E., Dean, D., Turgut, Z., Drummy, L., Mirau, P., Vaia, R., 2005. Generating triaxial reinforced epoxy/montmorillonite nanocomposites with uniaxial magnetic fields. Chem. Mater. 17, 1990–1996.

Kojima, Y., Usuki, A., Kawasumi, M., Okada, A., Kurauchi, T., Kamigaito, O., 1993a. Synthesis of nylon 6-clay hybrid by montmorillonite intercalated with ε-caprolactam. J. Polym. Sci. A Polym. Chem. 31, 983–986.

Kojima, Y., Usuki, A., Kawasumi, M., Okada, A., Kurauchi, T., Kamigaito, O., 1993b. One-pot synthesis of nylon 6-clay hybrid. J. Polym. Sci. A Polym. Chem. 31, 1755–1758.

Lagaly, G., 1979. The "layer charge" of regular interstratified 2:1 clay minerals. Clay Clay Miner. 27, 1–10.

Lagaly, G., 1981. Characterization of clays by organic compounds. Clay Miner. 16, 1–21.

Lagaly, G., 1986. Interaction of alkylamines with different types of layered compounds. Solid State Ion. 22, 43–51.

Lan, T., Pinnavaia, T.J., 1994. Clay-reinforced epoxy nanocomposites. Chem. Mater. 6, 2216–2219.

Li, Y., Zhao, L., 2011. Highly ordered hierarchical poly(ethylene oxide)-b-polystyrene/organoclay nanocomposites. ACS Appl. Mater. Interfaces 3, 1613–1619.

Liu, M., Ishida, Y., Ebina, Y., Sasaki, T., Hikima, T., Takata, M., Aida, T., 2015. An anisotropic hydrogel with electrostatic repulsion between cofacially aligned nanosheets. Nature 517, 68–72.

Na, Y.H., Aburaya, Y., Orihara, H., Hiraoka, K., Han, Y., 2014. Electrically induced deformation in chiral smectic elastomers with different domain structures. Phys. Rev. E 90, 062507.

Niskanen, E., 1964. Reduction of orientation effects in the quantitative X-ray diffraction analysis of kaolin minerals. Am. Mineral. 49, 705–714.

Ortiz, C., Wagner, M., Bhargava, N., Ober, C.K., Kramer, E.J., 1998. Deformation of a polydomain, smectic liquid crystalline elastomer. Macromolecules 31, 8531–8539.

Park, J.U., Choi, Y.S., Cho, K.S., Kim, D.H., Ahn, K.H., Lee, S.J., 2006. Time-electric field superposition in electrically activated polypropylene/layered silicate nanocomposites. Polymer 47, 5145–5153.

Patil, N., Balzano, L., Portale, G., Rastogi, S., 2009. Influence of nanoparticles on the rheological behaviour and initial stages of crystal growth in linear polyethylene. Macromol. Chem. Phys. 210, 2174–2187.

Pinnavaia, T.J., 1983. Intercalated clay catalysts. Science 220, 365–371.

Rao, Y., Blanton, T.N., 2008. Polymer nanocomposites with a low thermal expansion coefficient. Macromolecules 41, 935–941.

Schexnailder, P., Schmidt, G., 2009. Nanocomposite polymer hydrogels. Colloid Polym. Sci. 287, 1–11.

Sheng, N., Boyce, M.C., Parks, D.M., Rutledge, G.C., Abes, J.I., Cohen, R.E., 2004. Multiscale micromechanical modeling of polymer/clay nanocomposites and the effective clay particle. Polymer 45, 487–506.

Sun, T., Chen, F., Dong, X., Zhou, Y., Wang, D., Han, C.C., 2009. Shear-induced orientation in the crystallization of an isotactic polypropylene nanocomposite. Polymer 50, 2465–2471.

Urayama, K., Kohmon, E., Kojima, M., Takigawa, T., 2009. Polydomain-monodomain transition of randomly disordered nematic elastomers with different cross-linking histories. Macromolecules 42, 4084–4089.

Vaia, R.A., Teukolsky, R.K., Giannelis, E.P., 1994. Interlayer structure and molecular environment of alkylammonium layered silicates. Chem. Mater. 6, 1017–1022.

Velev, O.D., 2004. In: Schwartz, J.A., Contescu, C., Putyera, K. (Eds.), Electrically Functional Nanostructures, Chapter in Encyclopedia of Nanoscience and Nanotechnology. Marcel Dekker, New York, p. 1025.

Wang, K.H., Choi, M.H., Koo, C.M., Choi, Y.S., Chung, I.J., 2001. Synthesis and characterization of maleated polyethylene/clay nanocomposites. Polymer 42, 9819–9826.

Yano, K., Usuki, A., Okada, A., Kurauchi, T., Kamigaito, O., 1993. Synthesis and properties of polyimide-clay hybrid. J. Polym. Sci. A Polym. Chem. 31, 2493–2498.

Zanetti, M., Camino, G., Canavese, D., Morgan, A.B., Lamelas, F.J., Wilkie, C.A., 2002. Fire retardant halogen-antimony-clay synergism in polypropylene layered silicate nanocomposites. Chem. Mater. 14, 189–193.

Zevin, L., Viaene, W., 1990. Impact of clay particle orientation on quantitative clay diffractometry. Clay Miner. 25, 401–418.